NASA TECHNICAL MEMORANDUM

NASA TM-75048

(NASA-TM-75048) THE MODEL OF THE COMPOSITION OF THE MARTIAN ATMOSPHERE (National Aeronautics and Space Administration) 40 p HC A03/MF A01 CSCL 03B

N78-28028

Unclas

G3/91 26155

THE MODEL OF THE COMPOSITION OF THE MARTIAN ATMOSPHERE

M. N. IZAKOV AND O. P. KRASITSKIY

Translation of "Model' Sostava Atmosfery Marsa," Academy of Sciences USSR, Institute of Space Research, Moscow, Report Pr-320, 1977, pp. 1-37

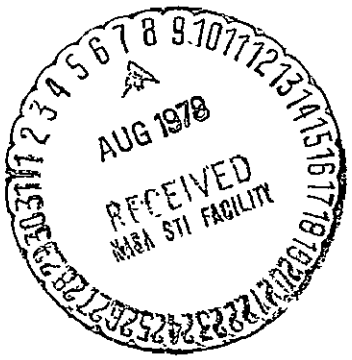

NATIOANAL AERONAUTICS AND SPACE ADMINISTRATION
WASHINGTON, D.C. 20546 OCTOBER 1977

STANDARD TITLE PAGE

1. Report No. NASA TM-75048	2. Government Accession No.	3. Recipient's Catalog No.
4. Title and Subtitle THE MODEL OF THE COMPOSITION OF THE MARTIAN ATMOSPHERE		5. Report Date October 1977 6. Performing Organization Code
7. Author(s) M. N. Izakov and O. P. Krasitskiy		8. Performing Organization Report No. 10. Work Unit No.
9. Performing Organization Name and Address Transemantics, Inc. 1901 Pennsylvania Avenue, NW Washington, DC 20006		11. Contract or Grant No. NASw-2792 13. Type of Report and Period Covered Translation
12. Sponsoring Agency Name and Address National Aeronautics and Space Administration Washington, DC 20546		14. Sponsoring Agency Code

15. Supplementary Notes

Translation of "Model' Sostava Atmosfery Marsa," Academy of Sciences USSR, Institute of Space Research, Moscow, Report Pr-320, 1977, pp. 1-37.

16. Abstract

Global mean distributions of Martian atmospheric components concentrations from the planet's surface up to an altitude of 250 km are calculated. Improved data on the turbulent mixing coefficient, as a function of altitude, on temperature distribution and on chemical and photochemical reaction rates are used.

The model data agree well with available measurements of some components concentrations. Variations of composition due to long-period variations of temperature, moisture and turbulent mixing are investigated. The relative significance of different catalytic cycles and the important role of excited atoms O (^{1}D) are revealed.

17. Key Words (Selected by Author(s))	18. Distribution Statement
	Unclassified-Unlimited

19. Security Classif. (of this report)	20. Security Classif. (of this page)	21. No. of Pages	22.
Unclassified	Unclassified	34	

THE MODEL OF THE COMPOSITION OF THE MARTIAN ATMOSPHERE

M. N. Izakov, O. P. Krasitskiy

Introduction

A knowledge of the composition of the planet's atmosphere along /3.
with its thermal conditions and dynamics is necessary to understand the structure of the atmosphere and the processes that take place in it, as well as to solve the problems of the evolution of the atmosphere.

During the past few years we have noted considerable progress in the study of the Martian atmosphere, including its composition, to a significant degree because of research using spacecraft. (See, for example, reviews [1-4] where there is a detailed bibliography).

The Martian atmosphere (the average pressure at the planet's surface is 6 millibars, the average temperature is 220°K [1-5]) contains approximately 95% CO_2, 2-3% N_2 and 1-2% Ar [6-7]. A large quantity of argon, obtained by indirect means [8], is either excessive or belongs to some kinds of local conditions. In addition, the atmosphere contains small components (the volumetric content relative to CO_2): molecular oxygen O_2 $(0.35-1.2)10^{-3}$; carbon monoxide CO- $(0.4-3.0)10^{-3}$. The content of water vapor in the atmosphere changes with the seasons and the latitude within the limits of approximately 5 to 50 μ of the precipitated water, and sometimes over the polar caps it falls to a fraction of a μ, and in lower latitudes it sometimes reaches 100 μ [13-17]. In the Martian atmosphere ozone is found; according to data of the ultra-violet spectrometers on the Mariner 6, 7 and 9 spacecrafts in the low latitudes, the level of O_3 /4. was less than the sensitivity level of the device, equal to 3 μ-atm.

(1 μ-atm. ≒ $2.687 \cdot 10^{15} cm^{-2}$), and in the polar areas the level of O_3 varied from 3 to 15 μ-atm., and sometimes reached 60 μ-atm. [18-19]. According to similar measurements on the "Mars-5" spacecraft, it was determined that in low latitudes the content of O_3 is not less than 3 μ-atm. and that the maximum of the layer of O_3 is located at approximately 40 kilometers [20]. The concentration of atomic hydrogen at altitudes of 200-250 km (measured by the luminescence of the atmosphere in the lyman-alpha line of hydrogen 1216 Angstroms) is equal to $n_H(250) \doteq (2-3) \cdot 10^4 cm^{-3}$ [21-24]. From the emissions of the Martian atmosphere in the lines of atomic oxygen we found that at an altitude of 135 km (close to the ionospheric maximum) the concentration of the atomic oxygen in relationship to the concentration of CO_2 is equal to $n_O(135) = 0.5-3\% \, n_{CO_2}$ [25-28]. From the emissions in the CO zones we made the following evaluation: $n_{CO}(135) = 0.3-1.0\% \, n_{CO_2}$ [26].

Theoretical models of the composition of the Martian atmosphere, permit in the first place, the coordination of different experimental data; secondly, prediction of the presence and altitude profiles of several atmospheric components that still have not been found in the experiments; thirdly, explanation of the surprising fact of the predominance of CO_2 to high altitudes in the presence of its quick photodissociation and slow association of CO and O [29-32]. However, several hypotheses formulated when constructing these models need to be refined, not all of the computed concentrations concur with the experimental data and have significant differences between the data from different models.

In this report we suggest a model of average global distributions of the atmospheric components from the surface to an altitude of 250 km,.

in which we used a more accurate turbulent mixing coefficient, depending on the altitude; we have refined the rates of several chemical reactions and the rates of photodissociation of several components according /5. to the latest experimental data; we used data obtained by us earlier on the thermal condition of the upper atmosphere; we developed a detailed method of computations. As a result we have a good agreement between the data of the models and all of the experimental data; we have explained possible variations in the concentrations of atmospheric components at different altitudes depending on the possible variations (long periods, for example - seasonal), the temperature, the humidity and the turbulent mixing; we have defined the relative role of the different processes determining the atmospheric composition of Mars. Limitations with long period variations are determined by the fact that we have found steady-state distribution of the concentrations under global-average conditions. However, since these distributions are determined by integration in time, this subsequently permits the use of the model apparatus after modernizing it for studying both short-term (daily) and longer period (evolutionary variations in the Martian atmospheric composition.

1. Construction of the Model

Spatial distributions and temporary variations of atmospheric components are described in equations of continuity for the concentrations of the components which include the basic processes determining the composition of the process - the origination and destruction of particles in chemical and photochemical reactions and their transfer by molecular diffusion and turbulent mixing (see, for example, [4]). The composition is of course

connected with the thermal conditions and movements in the atmosphere, so that a strict examination requires simultaneous solving of the continuity equations with the equations of movement and energy balance. However, in view of the fact that the basic component in the Martian atmosphere is CO_2 which prevails to high altitudes, we can initially find the thermal conditions and movements for the atmosphere from CO_2 (as it was done in [33]) and, using the temperature /6. profiles found there, we can solve the system of continuity equations for the components.

An evaluation of the characteristic times of the different processes which determine the planet's atmosphere show that the distribution of the components $n_\kappa(Z)$ at the altitude are basically determined by slower processes of transfer along the vertical, whereas the quick transfer along the horizontal (which is a result of the quasi-horizontality of atmospheric movements) to a significant degree decreases the daily variations. This fact allows us to ignore the derivatives along the horizontal in the transfer member and, thereby, to reduce the problem to a spatial-unidimensional one, having written the equation of continuity for concentrations of the components n_κ in the following form:

$$\frac{\partial n_\kappa}{\partial t} + \frac{\partial}{\partial z}\left[-D_\kappa n_\kappa\left(\frac{\partial \ln n_\kappa}{\partial z} + \frac{\mu_\kappa g}{R_0 T} + (1+\alpha_\kappa)\frac{\partial \ln T}{\partial z}\right)\right] + \tag{I}$$

$$+ \frac{\partial}{\partial z}\left[-K n_\kappa\left(\frac{\partial \ln n_\kappa}{\partial z} + \frac{\bar{\mu} g}{R_0 T} + \frac{\partial \ln T}{\partial z}\right)\right] = P_\kappa - L_\kappa$$

Here, t - time, Z - the altitude; D_k - the diffusion coefficient of the particles of the K-component, K - the coefficient of the turbulent mixing; T is the temperature; μ_k is the molecular weight of the k-component, $\bar{\mu}$ is the average molecular weight ($\bar{\mu}=n^{-1}\Sigma\mu_k$ n_x, $n=\Sigma n_k$), α_k is the thermodiffusion factor (significant only for hydrogen, $\alpha_{k_H}=0.38$); R_o is the universal gas constant; g is the acceleration of the force of gravity; P_k and L_k are the speeds of the appearance and disappearance of the particles of the k-component in the photochemical and chemical reactions.

The members describing the photodissociation of the molecules of the ℓ-type take on the form (see, for example, [4, 34]):

$$L_\ell = n_\ell \int \frac{F_{\lambda\infty}}{h\nu} \sigma_\ell^g \exp\left(-\int_z^\infty \Sigma\sigma_\ell n_\ell \sec\chi\, dz'\right) d\lambda = n_\ell J_\ell, \quad (22)$$

/7.

where λ, ν are the wave length and the photon frequency, X is the zenith angle of the sun, h is the Planck constant, $F_{\lambda\infty}$ is the spectral stream of the solar ultraviolet radiation on the boundary of the atmosphere (the values of which are used in accordance with [35], for $\lambda<1000$ Å, and according to [36], for large λ); σ_ℓ is the absorption coefficient by the ℓ-molecules, σ_ℓ^g is the photodissociation coefficient, equal to $\sigma_\ell^g=\sigma_\ell$ when $\lambda \geq 1000$ Å and $\sigma_\ell^g=\sigma_\ell-\sigma_\ell^i$ when $\lambda \leq 1000$ Å (here σ_ℓ^i is the ionization coefficient); the values of σ_{CO_2} are according to [37-39], of σ_{O_2} according to [36, 40, 41], σ_{O_3} according to [36], σ_{H_2O} according to [42], $\sigma_{H_2O_2}$ according to [43], σ_{HO_2}

according to [44].

The cross-section of the attenuation of radiation with carbon dioxide gas σ_{CO_2} quickly decreases the wave length λ up to $\lambda = 2050$ Å, and with larger λ it decreases much more slowly [38]. Shemansky [38] showed that this deviation on the $\sigma_{CO_2}(\lambda)$ curve is explained by the fact that here a cross-section of Rayleigh scattering is added to the cross-section of the absorption of photons in the process of photodissociation. Therefore, during computations of CO_2 photolysis we integrated up to $\lambda = 2050$ Å. If we consider the entire cross-section of attenuation due to photodissociation, then the rate of photolysis at the surface of Mars is an order of a magnitude greater.

In computing L_{CO_2}, L_{O_2}, L_{H_2O} (in an effective spectral interval $\lambda \lesssim 2050$ Å), in the sum, found in the index of the exponent in formula (2), only the member which takes CO_2 into consideration is essential (in view of its predominance), and the integral along Z is replaced by $N_{CO_2} = n_{CO_2}(Z)\, H_{CO_2}(Z)\sec X$ (since CO_2 is distributed according to the barometric formula). Thus, it seems that these members are the functions of the number of CO_2 molecules in the N_{CO_2} column. These functions can be solved beforehand, having been eliminated from integration for λ and for Z in each step of the computation. On the other hand, when calculating L_{O_2}, L_{H_2O}, L_{HO_2} (in the spectral interval $\lambda \lesssim 2000$ Å, where the cross-sections of these components are much larger than the CO_2 cross-sections and are comparable among themselves), all of them are included in the sum in the index of the exponent; in addition, the distributions of these components differ from the barometric formula; /8.

therefore, when computing these members one has to integrate both for Z and for λ.

To determine the average global distributions of $n_k(Z)$ we set the average daily profiles T(Z) according to [3, 33] and the average values for the photodissociation rates $\bar{L}_\ell$, for which we solve it when $X=60°$ and we take ½ of the resulting value to find out that the source is acting for one half the time of day, i.e. $\bar{L}_\ell = \frac{1}{2} L_\ell$ $(X \leqslant 60°)$. An examination of the previous models (including models for the composition of the Earth's upper atmosphere) and of our model of the thermal conditions of the Martian thermosphere shows that the average distributions found in this way are close to the conditions near the terminator in the middle latitudes.

The members describing the binary chemical reactions have the form: $K_s n_k n_\ell$, and the triple reactions: $- K_s n_k n_\ell n$. The accepted system of the reactions and the coefficients of the reaction speeds, chosen from the latest laboratory measurements and evaluations [45-62], are presented in table 1, which demonstrates the majority of K_s changes sharply depending on the temperature.

The model includes 12 neutral components: CO_2, O_2, CO, O_2, $O(^3P)$, $O(^1D)$, H, H_2, H_2O, OH, HO_2, H_2O_2, and also the ions CO_2^+, CO_2H^+. And for 11 components the system of equations (I) was solved, and the concentration of CO_2 was found from the barometric formula $n_{CO_2}(Z = 0)$ and T(Z), according to the model [3, 33]. Evaluations showed that this is a very close approximation, because, in the first place, the characteristic time for existence of CO_2 in the Martian atmosphere is very large, many orders of magnitude larger

than the characteristic time provided in the problem, and, in the second place, the CO_2 concentration is much larger than the concentrations of other components in almost all areas, and at high altitudes where the O concentration approximates that of CO_2, the diffusion time is so small that n_{CO_2} is determined by its concentration in the lower layers, so that the barometric formula for it is not impaired for all practical purposes. /9.

The ion reactions [34, 35] (table 1) significantly affect the concentration of the neutral hydrogen n_H at altitudes greater than ~100 km. The CO_2^+ concentration was taken close to the empiric profiles, according to the measurements of the "Viking" spacecraft [12].

The expressions for the diffusive streams in a multi-component mixture of gases are very complex [63, 64], however, the predominance of CO_2 in the Martian atmosphere allows us to use an approximation of the small component, by using D_k - the diffusion coefficients of the k-component in CO_2 where D_k is very well approximated in the form $D_k = AT^S n^{-1}$. The expressions D_k for the components in the computations are taken from experimental data [65, 66], and for several molecules for which there are no data, they are taken from the molecular characteristics, presented in [63, 64]; moreover, for these molecules of the short-lived components, D_k is completely insignificant (in view of the presence of photochemical balance $P_k = L_k$).

The turbulent mixing coefficient K was given as an altitude function in the following manner: we considered that near the homopause the values of K can change from $K_1 = 9.10^6$ to $8.10^7 cm^2 sec^{-1}$,

according to the estimates [67]; then the altitude of the homopause changes from Z_1=120-240 km; at the planet's surface the values for K can change from $K_0=10^5-10^6 cm^2 sec^{-1}$ [68-69]; from the surface to the homopause we considered that log K increases linearly (see figures 1-4 and table 2).

In computing the models we assigned the following boundary conditions: on the lower boundary (at the planet's surface, where Z = 0) we assigned the absence of streams for all components, except /10.
H_2O. For water vapors we assigned a definite value of the concentration $n_{H_2O}(0)$, starting from the assigned humidity which, for different variations of the model, changes from 0.6 to 70μ of precipitated water in accordance with the experimental data [16, 17]. At the upper boundary (Z = 250 km) we assigned the condition of diffusive equilibrium for all components, except H, H_2 and O. For H and H_2 we used the departing stream because of the thermal dissipation, according to the Jean formula:

$$\Phi_{H,H_2} = \left(\frac{KT}{2\pi m}\right)^{1/2} (1+X_c)\, exp(-X_c)\cdot n_{H,H_2}, \qquad (3)$$

where K is the Boltzman constant, subscript c is the value of the exobase $X = \frac{r}{H_{H,H_2}}$. For oxygen we used the departing stream, equal to half the departing stream of the atomic hydrogen, i.e. $\Phi_O = \frac{1}{2}\left(\Phi_H + 2\Phi_{H_2}\right)$ in accordance with the McElroy conclusion on the presence of nonthermal escape of oxygen as a result of the fact that during the dissociation-recombination reactions $CO_2^+ + e \rightarrow CO + O$ и $O_2^+ + e \rightarrow O + O$, the O atoms obtain a

speed larger than the critical speed [30, 70]. The estimates of the number of atoms with velocities higher than the critical, forming in the dissociation-recombination reactions, are also close to the Φ_o value.

The choice of the initial conditions of n_{CO} and n_{O_2} is made according to empirical data and is based on the following considerations. The dominant components of the Martian atmosphere enter into reactions as a result of which (ignoring several secondary reactions) can be written as $2CO_2 \rightleftarrows 2CO + O_2$, i.e. for each O_2 molecule, two CO molecules are formed and disappear or $\Delta N_{CO} \approx 2\Delta N_{O_2}$ and consequently, $N_{CO} \approx 2N_{O_2} + A$, where A is a constant.*) If A = 0 (i.e. at the initial moment the Martian atmosphere would have consisted /11. of pure CO_2), then it would always be that $N_{CO}/N_{O_2} \approx 2$. However, the experiments show that in the Martian atmosphere the value of this relationship lies within the limits of 0.5-1.0. As initial conditions for CO and O_2 we also chose the latter profiles, so that constant $A = -2.12 \cdot 10^{20} cm^{-2}$ (a certain excess of O atoms is assigned). In this case with $N_{CO} = 2.12 \cdot 10^{20} cm^{-2}$ we get $N_{O_2} = 2.12 \cdot 12^{20} cm^{-2}$ and $N_{CO_2}/N_O = 1$, which is close to the experimental data. The computations showed that in all variations of the model the relationship $N_{CO}/(2N_{O_2} + A) \approx 1$ with good accuracy (the deviations do not exceed 4%, see table 2). This shows that at first this difference in the inflow and outflow of water does not lead to a significant accumulation of O_2 in the Martian atmosphere and, secondly - the computation scheme is conservative.

*) The relationship $2\Delta C = \Delta O$ is a little more accurately fulfilled (locally), which may be verified by writing their equality thusly:
$2f_{O_2} + 3f_{O_3} + f_{H_2O} + 2f_{H_2O_2} + f_O + f_{OH} + 2f_{HO_2} + f_{O(^1D)} - f_{CO} = 0$
and substituting the expression for $f_k = P_k - L_k$. However, even this equality is impaired (integrally) because of the differences between

2. Numerical Method

For a numerical solution the initial system of equations (I) is written as:

$$\frac{\partial n_k}{\partial t} = \frac{\partial}{\partial z}\left[(D_k + K) y_k \frac{\partial}{\partial z}\left(\frac{n_k}{y_k}\right)\right] + P_k - L_k \quad (4)$$

where $y_k(Z)$ is the steady-state solution of the boundary problem with zero streams on the border, with arbitrary initial conditions and zero P_k and L_k.

$$y_k(z) = C \exp\left\{-\int_0^z \left[\frac{1}{T}\frac{\partial T}{\partial z} + \frac{D_k \bar{H} + K H_k}{H_k \bar{H}(D_k + K)}\right] dz\right\} \quad (5)$$

/12.

The constant C is determined by selected initial conditions. The expression (5) is a generalization of the barometric formula for the k-component. Writing the equation in the form (4) permits the isolation of the exponential dependence of the concentration on the altitude, which significantly improves the differential approximation of the initial system of differential equations, because many components of the Martian atmosphere are distributed according to the barometric formulas O_2, H_2O, CO, H_2 at all intervals of the altitudes, H and O in the upper layer of the atmosphere).

A stationary solution is sought by the determination method, i.e. we are integrating for t until we find a stationary solution. Differential equations are replaced by the differences on a network

---

the amount of O atoms leaving the atmosphere. Precisely because of this there is an excess of O_2 in the Martian atmosphere, described herein with the constant A.

of uneven altitudes (with thickening at the bottom). In most of the computations we used the following network: Z_i = 0, 0.1, 0.3, 0.9, 2.7, 6.4, 12.5, 18.7, 25, 32, 39, 47, 60, 74, 91.2, 105, 120, 140, 160, 200, 250 km. Such a concentration of points is made for improving the approximation of the system of diffusion equations by the differences at a set number of points and for decreasing the possible error because of the poor approximation of the lower limiting border condition (zero stream).

We use a conservative, unclear differential scheme of the second order of accuracy for Z: the diffusion member is written along three points corresponding to [71], but the nonlinear members are aligned in the middle point and at each intermittent step they are improved by iterations according to the Newton method. The solution of linear equations at each iteration is conducted jointly by the exclusion method of Gauss. Thus, the differential scheme takes the form:

$$\frac{{}^{p+1}n^{j+1}_{K,m} - n^{j}_{K,m}}{\Delta t} + \frac{{}^{p+1}q^{j+1}_{K,m+1/2} - {}^{p+1}q^{j+1}_{K,m-1/2}}{\Delta Z_m} = {}^{p}f^{j+1}_{K,m} + \sum_{\beta}\left[\frac{\partial f_K}{\partial n_\beta}\right]^{j+1}_{m}\left({}^{p+1}n^{j+1}_{\beta,m} - {}^{p}n^{j+1}_{\beta,m}\right),$$

/13.

here $\{Z_m, m = 0.1,\ldots N,\ Z_0 = 0,\ Z_N = 250$ km, $\Delta Zm = Zm - Zm-1\}$ is an uneven network.

m is the number of the point by the altitude; $\overline{\Delta Zm}$ is the step by altitude;

ν is the number of steps in time; Δt is the step in time;

P is the number of iteration by nonlinearity;

K is the number of the component;

$$Z_{m-1/2} = Z_m - 0.5 \cdot \Delta Z_m ,$$

$$Z_{m+1/2} = Z_m + 0.5 \cdot \Delta Z_{m+1} ,$$

$$\overline{Z_m} = 0.5 \cdot (\Delta Z_m + \Delta Z_{m+1}) ,$$

$$a_{m+1/2} = [(D_K + K) y_K]_{m+1/2} ,$$

$$a_{m-1/2} = [(D_K + K) y_K]_{m-1/2} ,$$

$$q_{yK,m+1/2} = -a_{m+1/2} \frac{\left[\frac{\Pi_K}{y_K}\right]_{m+1} - \left[\frac{\Pi_K}{y_K}\right]_m}{\Delta Z_{m+1}} ,$$

$$q_{yK,m-1/2} = -a_{m-1/2} \frac{\left[\frac{\Pi_K}{y_K}\right]_m - \left[\frac{\Pi_K}{y_K}\right]_{m-1}}{\Delta Z_m}$$

-- the expression for diffusive streams.

To obtain a conservative differential scheme we must also write out the differential expressions for diffusive streams on the boundaries. The following expressions maintain the conservatism of the scheme:

$$q_{K,\,N-1/2} = 0$$ - on the upper boundary;

$$q_{K,\,1/2} = 0$$

$$q_{H,N-1/2} = \Phi_H(z_c)$$ - on the lower boundary.

$$q_{H_2,N-1/2} = \Phi_{H_2}(z_c),$$

$$q_{O,N-1/2} = \frac{1}{2}\Phi_H(z_c) + \Phi_{H_2}(z_c)$$ /14.

The boundary condition for H_2O at the lower boundary is written as: $n_{H_2O,\,0} = C_1$, where C_1 is the assigned concentration.

In view of the large scatter of characteristic times

$$\left(\tau_{chem} = \left[\frac{\partial f_K}{\partial n_K}\right]^{-1} = 10^{-8} - 10^{10}\ \text{sec},\quad \tau_{dif} = 10^2 - 10^7\ \text{sec}\right)$$

the linear differential system of equations, approximating the system of differential equations, is poorly stipulated. The poor stipulation leads to an increase in errors in rounding off with the growth of Δt. In conjunction with this at large times (larger than approximately 10^7 sec) we had to compute with double accuracy (Fortran BESM-6, twenty-four decimal places). Since the number of required operations for solving the system of equations according to the Gauss method is proportional to the cube of the number of equations, the multiple components of the problem also lead to serious difficulties.

To overcome the difficulties we used the following scheme of computations:

1. From the initial conditions we make one step in time $\Delta t \sim 0.1$ sec.;

if the iterations coincide, Δt is increased by a factor of 1.5; if the iterations do not coincide (since at the given Δt sharp changes in n_k take place), the step is decreased by 3 times; these computations are conducted on a coarse network - ten points along the altitude.

2. With the appearance of large errors in rounding off (they appear because at the given Δt the concentrations n_k change very little which is confirmed by the integrating at the point of time Δt with a small step Δt; the iterations nevertheless do not coincide - the significant numbers n_k "dangle") the computations are continued with double accuracy on the BESM-6 computer the speed of the computation is decreased by 4-5 times); the computations are also continued on the coarse network.

3. After obtaining the steady solution on the coarse network the number of points increases until we obtain the necessary accuracy (21 points were sufficient to arrive at 5% accuracy). /15.

Receiving a steady solution with this set of computations takes $\sim$ 1 hour.

After this we vary T, N_{H_2C}, K - the time for solving different variations is $\sim$ 6 minutes (time for first iteration at the 21st point on the altitude with double accuracy is $\sim$1.5 minutes).

In conclusion, we can say that the numerical method was practical in solving the problems with the number of components in the order of ten. This method is the strictest, does not use the specifics of the chemical and diffusion processes and therefore is most general. Of course, other methods of solution are possible,

which use the specifics of the processes and therefore can be more economical. For example, in the work [73, 74] the component cleavage of the chemical processes is used and the correction of the solution takes place by examining the groups of active components, the concentration of which slowly changes in time. The work [72] uses the cleavage of the physical processes, i.e. the diffusion is separated from the chemistry. After this, the diffusion equations are cleaved by component and are solved by subsequent scalar trial runs, and the equations of chemical kinetics are solved jointly.

3. Results and Discussion

The altitude distribution of the concentrations n_k in several basic variations of the model are presented in figures 1-4 and, in addition, the basic characteristic of several of the variants are presented in table 2, where the available experimental data are presented. The figures show that the long-lived components (CO_2, CO, /16.
O_2, H_2, H_2O) are distributed in the altitude according to the barometric formula, whereas in the homosphere the altitude scale is the same for all of the components, and in the heterosphere - they are different; in the water vapor in the troposphere the altitude scale is determined by the curve of saturation and is approximately equal to 2 km, which is significantly less than $\bar{H}$. The remaining short-lived components have more complicated profiles, and the profiles $O(^3P)$, $O(^1D)$, H and OH have maximums at the planet's surface. $[CO_2]$ is comparable with [O] at Z=250 km. (in the basic variation).

2. Let us compare the characteristics of our model with the experimental data which, as we showed in the introduction, are quite numerous and varied. As we see from table 2, the values of the total content of O_2 and CO in most variations of the model are within the limits of the distribution of the experimental data, with the exception of low-humidity variation (0.6 μ of precipitated water), which yields somewhat larger values. The values of the relative concentrations $[O]/[CO_2]$ and $[CO]/[CO_2]$ on the ionospheric maximum are also within the distribution field of the experimental data except for the variant with the minimal turbulent mixing coefficient in the thermosphere ($K_1 = 9 \cdot 10^6 cm^2/sec$), which yields values that are several times larger. It is entirely possible that there variants may be realized also at some time.

The values for the concentration of atomic hydrogen on the upper boundary at an increased temperature T_∞ and decreased humidity approximate the experimental values $[H]_{250} = (2 - 3) \cdot 10^4 cm^{-3}$, but in most of the variants they exceed these values several times. The basic model satisfies the experimental data best of all (the average for K in the upper atmosphere and the minimal in the lower atmosphere). In this model all of the concentrations lie within the limits of /17. the scatter zone of the experimental data, except a slightly increased content of O_3 (7.4 μ-atm.) and a slightly increased $[H]_{250} = 3.7 \cdot 10^4 cm^{-3}$.

The ozone concentrations in our model change from 21 μ-atm. at low humidity (equal to 0.6 μ of precipitated water) to 4.7 μ-atm. O_3 at 15 μ or more of precipitated water (figure 5). These values are within the scatter limits of the experimental data (3-60 μ-atm. O_3).

True, the values at high humidity (approximately 5 μ-atm.) are slightly higher than the experimental ($\lesssim$3 μ-atm), however, it was found that complete agreement is obtained if we take a warmer troposphere; this is completely cut, i.e. in our model we took the global, average value at the surface of the planet T_o = 220 K, whereas at the lower latitudes where there is a lot of humidity [16, 17], significantly higher temperatures T_o = 250 - 270°K are usual [3, 5, 75]. The ozone content at the increased temperature increases because of the reverse temperature dependence of the speed of the reaction K_{ii}.

This permits us to conclude that the data of our model are in good agreement with all of the available experimental data.

3. The model shows that the variations in intensity of the turbulent mixing in the thermosphere within the possible limits (K_i = 9.10^6-$8.10^7 cm^2 sec^{-1}$) result in noticeable variations of the concentrations of several components (compare the variations 2 and 3 in table 2). The O and CO concentrztions decrease especially strongly with an increase in K (approximately by 6 and 3 times, respectively). Apparently this takes place as a result of an increase in the transfer of the CO_2 molecules upwards where they are subjected to photodissociation, and a transfer of CO and O downward where they associate as a result of the cycles of chemical reactions described below. Lower values of the H concentration at the exobase also correspond to a greater intensity of the turbulent mixing in the thermosphere. /18.

The turbulence in the lower atmosphere also plays an important

role. With the reduction of K the total content of CO, O_2, and O_3 increases and the level of H_2 declines, whereas the H and H_2 at the exobase decrease. In our model when $K_o = 10^5 cm^2 sec^{-1}$, in the troposphere the best concurrence with the experimental data is obtained.

4. Studies of the effect of the variations of temperature in the upper thermosphere (the average global values of which can vary from $\bar{T} = 262°K$ at low solar activity to $\bar{T}_\infty = 359°K$ at high solar activity [76]) shows (compare variants 4 and 5 of the model) that with an increase in T_∞ within the prescribed limitations, the concentrations of several components at high altitudes increase (for example, $[CO_2]_{250}$ increases by approximately 5 times) because of an increase in the altitude scale, and the concentrations of the atomic and molecular hydrogen noticeably decrease (by 5 and 1.6 times, respectively) because of an increase in the stream of the thermal dissipation, the effect of which prevails over the effect of an increase in the altitude scale.

5. The effect of the increase in the humidity is manifested, as we noted above, by a strong decrease in the ozone content (figure 5). In addition, with an increase in the humidity from 0.6 μ to 35 μ of the precipitation, the level of H, H_2 and OH significantly increases; thus, the concentrations at the upper boundary $[H]_{250}$, $[H_2]_{250}$ increase approximately 7 times, and the concentrations at the lower boundary $[OH]_o$ increase 10 times.

6. We studied the effect of the variations of the ion composition, or the amount of $[CO_2^+]$, on the concentration of the atomic hydrogen in the thermosphere. Since the hydrogen in the thermosphere

is basically formed in the reactions (34, 35), then with a decrease in $[CO_2^+]$ by 3 times, the concentration of $[H]_{250}$ decreases by 2 times (variants 9 and 10). /19.

7. The model shows that the effect of the reaction of the photodissociation predominates at altitudes higher than approximately 50 km, but in velocities the chemical relations are comparable with them at lower altitudes (figure 6). The difference between the speeds of formation and destruction of the components is compensated for by the diffusion streams below 120-140 km - as a result of the turbulent diffusion), which, as we see from figure 7, transfer the CO and O downward; O_2 is transferred upward at altitudes more than ~60 km and downward at lower altitudes; H - upward at altitudes more than ~105 km and downward at lower altitudes; H_2 - upward at altitudes more than approximately 20 km and downward at lower altitudes; O_3 - upward at altitudes more than 40 km and downward at lower altitudes.

Some of the reactions introduced by us turned out to be insignificant (7, 8, 12, 16, 21, 27, 29, 33), meaning that their contribution to the balance of any component in the entire range of altitudes examined is less than 1%. These reactions may be excluded from further computations.

In previous reports [2, 29 - 32], we indicated several catalytic cycles aiding the association of CO and O, specifically:

Ist cycle:

$$H + O_2 + M \rightarrow HO_2 + M$$

$$HO_2 + O \rightarrow OH + O_2$$

$$CO + OH \rightarrow CO_2 + H$$

---

resulting: $CO + O \rightarrow CO_2$

then the II cycle:

$$H + O_2 + M \rightarrow HO_2 + M$$

$$HO_2 + HO_2 \rightarrow H_2O_2 + O_2$$

$$H_2O_2 + h\nu \rightarrow 2OH$$

$$CO + OH \rightarrow CO_2 + H$$

---

resulting: $2CO = O_2 \rightarrow 2CO_2$ /20.

and, finally, the III cycle:

$$O + O_2 + M - O_3 + M$$

$$O_3 + H - OH + O_2$$

$$CO + OH - CO_2 + H$$

---

resulting: $CO + O - CO_2$

This yielded opposing opinions about the relative humidity of these cycles. Our model shows that all three cycles play a definite roles, and at the surface in the 2nd cycle 63% of the OH molecules form, in the 1st cycle - 35% and in the 3rd - approximately 1%; at an altitude of several km the prevailing contribution is given by the 1st cycle, the 2nd cycle becomes negligible; at an altitude of approxiamtely 30 km the 3rd cycle's contribution is comparable to that of the 1st cycle and at higher altitudes (up to 100 km) the 3rd cycle prevails.

An important role in the chemistry of the Martian atmosphere is played by excited oxygen $O(^1D)$ atoms in spite of the fact that

their concentration is very small (about 1 cm^{-3}). These atoms are formed in the photodissociation of O_3 (reaction 3) with a speed approximately of $1.1 \cdot 10^7 cm^{-3} sec^{-1}$, and immediately, approximately with the same speed, they are destroyed in the impact deactivation with CO_2 (No. 18), however, approximately $2 \cdot 10^4$ atoms $cm^{-3} sec^{-1}$, enetring reaction 19 effectively break up the hydrogen molecules and approximately $3.5 \cdot 10^2$ atoms $cm^{-3} sec^{-1}$ as a result of reaction 20 break up the H_2 molecule.

8. The global, daily-average streams of dissociating radiation which we used can increase the concentrations of the short-lived components. Therefore, we computed a variation (figure 4, No. 11 in table 2), in which we used the average daily L_{O_3}, $L_{H_2O_2}$ and L_{HO_2} (i.e. L_α ($X = 60^\circ$)), twice greater than the daily average. In this variation we obtained an ozone layer (N_{O_3} = 3.4 μ-atm.) close to the experimental level. It is also interesting that in this variation /21. (in comparison with variation No. 1) that the concentration of CO at the surface decreased two times, and the concentration of O_2 decreased 1.5 times, whereas in the thermosphere the concentration of all of these components practically does not change. Apparently, this decrease took place as a result of the cycles of chemical reactions mentioned above. Further improvement of this factor is possible onyl within the framework of a model describing the daily variations.

To compare our model with that of Liu and Donahue [32] we computed variation (no. 12 in table 2) with parameters close to those used in [32] ($K = 4 \cdot 10^8 cm^2 sec^{-1}$, N_{H_2O} = 15μ of the precipitated water, close profiles of $T(Z)$, $n_{CO_2}(Z)$). The concentration of most of the components in this variation satisfactorily agree with those in [32], and the

ratios of $[O]_{140}/[CO_2]_{140}$ and $[CO]_{140}/[CO_2]_{140}$ is almost one order less than that of [32]. The concentration of $[CO_2] = 1.65 \cdot 10^{-4} [CO_2]_o$ and $[O_2] = 6.10^{-4} [CO_2]_o$ are considerably lower than in [32] apparently because of lesser speed of the CO_2 photodissociation in our model, equal to $1.7 \cdot 10^{12} cm^{-2} sec^{-1}$ (see the speeds of the reactions in figure 5). In addition, it can be seen that in our model some additional conditions were not applied, which were used in [32].

10. Measurement s using the mass-spectrometer on the Viking spacecraft showed that present in the Martian atmosphere are nitrogen ($[N_2] \approx 2\text{-}6\% [CO_2]$) and nitrous oxide ($[NO] \approx 10^7 cm^{-3}$ at an altitude of 110 kilometers). Evaluations showed that these small concentrations of NO do not significantly alter the picture obtained from our model. However, the concentrations of several small components (particularly - HO_2) can change somewhat. Moreover, there is a possible effect of NO on the ionosphere through the reactions $N_2^+ + O \rightarrow NO^+ + N$ and $N_2^+ + NO \rightarrow NO^+ + NO_2$ which have high speeds in the order of $10^{-10} cm^{-3} sec^{-1}$.

11. For different variations of the described model we performed evaluations of the departing stream of oxygen atoms Φ_o arising with the dissociative recombination of the O_2^+ and CO_2^+ ions (an exact computation is possible only with an exact determination of the distribution of the ion concentration and the electron and ion temperatures). It turned out that the Φ_o is much less variable than the departing stream of hydrogen atoms ($\Phi_H + 2\Phi_{H_2}$) (because the first one is determined ultimately by the concentration of the basic component CO_2 and by the speed of the ion formation, whereas the second one depends more on the neutral composition and its variations). In several variations the ratio of these streams is entirely

/22.

$\Phi_0/(\Phi_H+2\Phi_{H_2}) \approx$ 0.2--- 0.3, that is less than 0.3, which was permitted earlier. It is possible because of this consideration over a long period of time to build up an excess of oxygen atoms, noted above (see page 11).*

In conclusion we would like to express our thanks to A.I. Poroykova (Institute of Chemical Physics, Academy of Sciences USSR), for help in selecting the coefficients of the speeds of the chemical reactions, E.E. Shnol (Institute of Applied Mathematics, Academy of SCiences USSR) for his consultation on the numerical methods and T.M. Donahue (University of Michigan) for familiarizing us with his report [32] before its publications.

---

* TN: Page number of the Russian text.

Table 1

No.	Reaction	Speed	Reference (*)
I.	$CO_2+h\nu(40\text{-}2062) \rightarrow CO+O$	$J_\infty = 3{,}62.10^{-7}$	[37,38,39]
2.	$O_2+h\nu(40\text{-}2062) \rightarrow O+O$	$2{,}00.10^{-6}$	[36,40,41]
3.	$O_3+h\nu(2000\text{-}3600) \rightarrow O(^1D)+O_2$	$4{,}12.10^{-3}$	[36]
4.	$H_2O+h\nu(1515\text{-}2000) \rightarrow OH+H$	$2{,}06.10^{-6}$	[42]
5.	$H_2O_2+h\nu(2000\text{-}3600) \rightarrow OH+OH$	$7{,}41.10^{-5}$	[43]
6.	$HO_2+h\nu(2000\text{-}3600) \rightarrow O+OH$	$5{,}65.10^{-4}$	[44]
7.	$CO + O + CO_2 \rightarrow CO_2 + CO_2$	$1{,}01.10^{-32}\exp(-\frac{2190}{T})$	[45,46]
8.	$CO + O \rightarrow CO_2 + h\nu$	$6{,}64.10^{-18}\exp(-\frac{1850}{T})$	[47]
9.	$CO + OH \rightarrow CO_2 + H$	$2{,}1.10^{-13}\exp(-\frac{116}{T})$	[48]
10.	$O + O + CO_2 \rightarrow O_2 + CO_2$	$3.10^{-33}\ (\frac{T}{300})^{-2,9}$	[49,50]
11.	$O + O_2 + CO_2 \rightarrow O_3 + CO_2$	$1{,}4.10^{-33}\ (\frac{300}{T})^{-2,5}$	[49,50]
12.	$O + O_3 \rightarrow 2O_2$	$2{,}0.10^{-11}\exp(-\frac{2280}{T})$	[51]
13.	$O + H_2 \rightarrow OH + H$	$7{,}0.10^{-11}\exp(-\frac{5000}{T})$	[50]
14.	$O + OH \rightarrow O_2 + H$	$4{,}0.10^{-11}$	[52,53]
15.	$O + HO_2 \rightarrow OH + O_2$	$8{,}0.10^{-11}\exp(-\frac{500}{T})$	[54]
16.	$O + H_2O_2 \rightarrow H_2O + O_2$	$2{,}3.10^{-11}\exp(-\frac{3200}{T})$	[55]
17.	$O + H_2O_2 \rightarrow OH + HO_2$	$2{,}3.10^{-11}\exp(-\frac{3200}{T})$	[55]
18.	$O(^1D)+ CO_2 \rightarrow O(^3P)+ CO_2$	$1{,}8.10^{-10}$	[56]
19.	$O(^1D) + H_2O \rightarrow 2OH$	$3{,}0.10^{-10}$	[57,58]
20.	$O(^1D) + H_2 \rightarrow OH + H$	$3{,}0.10^{-10}$	[57,58]

Table 1 continued:

21.	$H + HO_2 \rightarrow 2OH$	$4,2.10^{-10} \exp(-\frac{950}{T})$ [54]
22.	$H + HO_2 \rightarrow H_2O + O$	$8,3.10^{-11} \exp(-\frac{500}{T})$ [54]
23.	$H + HO_2 \rightarrow H_2 + O_2$	$4,2.10^{-11} \exp(-\frac{350}{T})$ [54]
24.	$H + O_2 + CO_2 \rightarrow HO_2 + CO_2$	$2,0.10^{-31} (\frac{T}{273})^{-1,3}$ [59]
25.	$H + H + CO_2 \rightarrow H_2 + CO_2$	$1,0.10^{-32} (\frac{T}{273})^{-0,7}$ [50]
26.	$H + O_3 \rightarrow OH + O_2$	$2,6.10^{-11}$ [60]
27.	$OH + OH \rightarrow H_2O + O$	$1,0.10^{-11} \exp(-\frac{550}{T})$ [52]
28.	$OH + H_2 \rightarrow H_2O + H$	$3,6.10^{-11} \exp(-\frac{2590}{T})$ [52]
29.	$OH + O_3 \rightarrow HO_2 + O_2$	$1,3.10^{-12} \exp(-\frac{956}{T})$ [61]
30.	$OH + HO_2 \rightarrow H_2O + O_2$	$8,3.10^{-11} \exp(-\frac{500}{T})$ [54]
31.	$OH + H_2O_2 \rightarrow H_2O + HO_2$	$4,1.10^{-11} T^{1/2} \exp(-\frac{600}{T})$ [62]
32.	$HO_2 + HO_2 \rightarrow H_2O_2 + O_2$	$1,7.10^{-11} \exp(-\frac{500}{T})$ [54]
33.	$H + OH \rightarrow H_2 + O$	$3,0.10^{-11} \exp(-\frac{4000}{T})$ [50]
34.	$CO_2^+ + H_2 \rightarrow CO_2H^+ + H$	$1,4.10^{-9}$ [32]
35.	$CO_2H^+ + e \rightarrow CO_2 + H$	$3,5.10^{-7}$ [32]

*) For J_ℓ - a reference to the source from which δ_ℓ are taken to compute J_ℓ. J_∞^ℓ - the value of J_ℓ at the boundary of the Martian atmosphere.

Variation No.	1	2	3	4	5	6
T , ^{o}K	322	322	322	359	262	322
$K_I(cm^2_{sec}{}^{-1}).10^{-7}$	3.0	8.0	0.9	8.0	8.0	8.0
$K_o(cm^2_{sec}{}^{-1}).10^{-6}$	0.1	1	1	1	1	1
$N_{H_2O}(\mu)$	15	15	15	15	15	0.6
$N_{O_2}\ (cm^{-2}).10^{-20}$	3.13	2.43	2.52	2.43	2.43	4.82
$N_{O_2}/N_{CO_2}.10^{+3}$	1.5	1.2	1.2	1.2	1.2	2.7
$N_{CO}(cm^{-2}).10^{-20}$	4.16	2.74	2.91	2.74	2.74	7.59
$N_{CO}/N_{CO_2}.10^{+3}$	2.2	1.3	1.4	1.3	1.3	4.2
$N_{O_3}(\mu\text{-atm})$	7.1	4.7	4.7	4.7	4.7	21
$[O]_{140}/[CO_2]_{140}.10^{+2}$	2.3	1.3	6.3	1.3	1.3	2.5
$[CO]_{140}/[CO_2]_{140}.10^{+2}$	1.8	1.1	3.2	1.1	1.1	2.0
$[H]_{250}(cm^{-3}).10^{-4}$	3.7	7.9	9.1	4.7	23	1.4
$[H_2]_{250}(cm^{-3}).10^{-5}$	2.4	5.2	5.5	4.1	6.7	0.89
$[H_2]_o(cm^{-3}).10^{-12}$	1.6	3.7	3.4	3.7	3.7	0.62
$[O_3]_o(cm^{-3}).10^{-9}$	6.5	5.0	5.1	5.0	5.0	54
$[HO_2]_o(cm^{-3}).10^{-8}$	4.7	3.8	3.9	3.8	3.8	3.0
$[H_2O_2]_o(cm^{-3}).10^{-9}$	12	6.1	6.5	6.1	6.1	4.6
$[O]_{max}(cm^{-3}).10^{-10}$	9.7	4.7	7.5	4.7	4.7	5.3
$[OH]_{max}(cm^{-3}).10^{-5}$	1.1	2.0	1.7	2.0	2.0	1.5
$[O(^1D)]_{max}\ (cm^{-3})$	3.1	2.1	2.2	2.1	2.1	3.3
N_{CO}/N_{O_2}	1.3	1.1	1.2	1.1	1.1	1.6
$N_{CO}/(2N_{O_2} + A)$	1.00	1.00	0.997	1.00	1.00	1.01

7	8	9	I0	II	I2	Model No. 32	Experimental data
322	322	322	322	322	322	320	
8.0	8.0	8.0	8.0	3.0	40	40	
I	I	I	I	0.I	40	40	
3.3	35	70	70	I5	I5	I5	
3.47	I.75	I.53	I.53	2.I2	I.23		
I.8	0.92	0.8	0.8	I	0.6	I.3	0.35 ~ 3.0
4.85	I.47	0.982	0.978	2.I4	0.336		
2.5	0.73	0.5	0.5	I	0.I6	I.6	0.4 ~ 3.0
8.8	4.7	4.2	4.2	3.4	5.2	2.2	up to 70
I.6	2	2	2	2.3	0.072	0.5	0.5 ~ 3
I.4	I.3	I.2	I.2	I.6	0.085	0.56	0.3 - I
3.7	9.5	II	6.4	4.7	2.5	3.I	2 ~ 3
2.5	6.I	7.3	I5	3	2.6	I.4	
I.7	4.3	5.I	5.5	2	3.9	2.2	
I5	5.6	4.I	4.I	2.9	I4	5	
3.4	5.I	5.8	5.8	4.7	2.3	2.5	
5.6	9.8	I2	I2	5.7	I	I.4	
4.6	4.7	4.7	5.I	I0	0.I7	0.I6	
I.8	3.9	3.7	3.8	I.3	7.3	I5	
3.4	I.7	I.5	I.8	3.0	0.88		
I.4	0.8	0.63	0.63	I.0	0.27	I.2	
I.0I	I.02	I.04	I.04	I.0I	0.988		

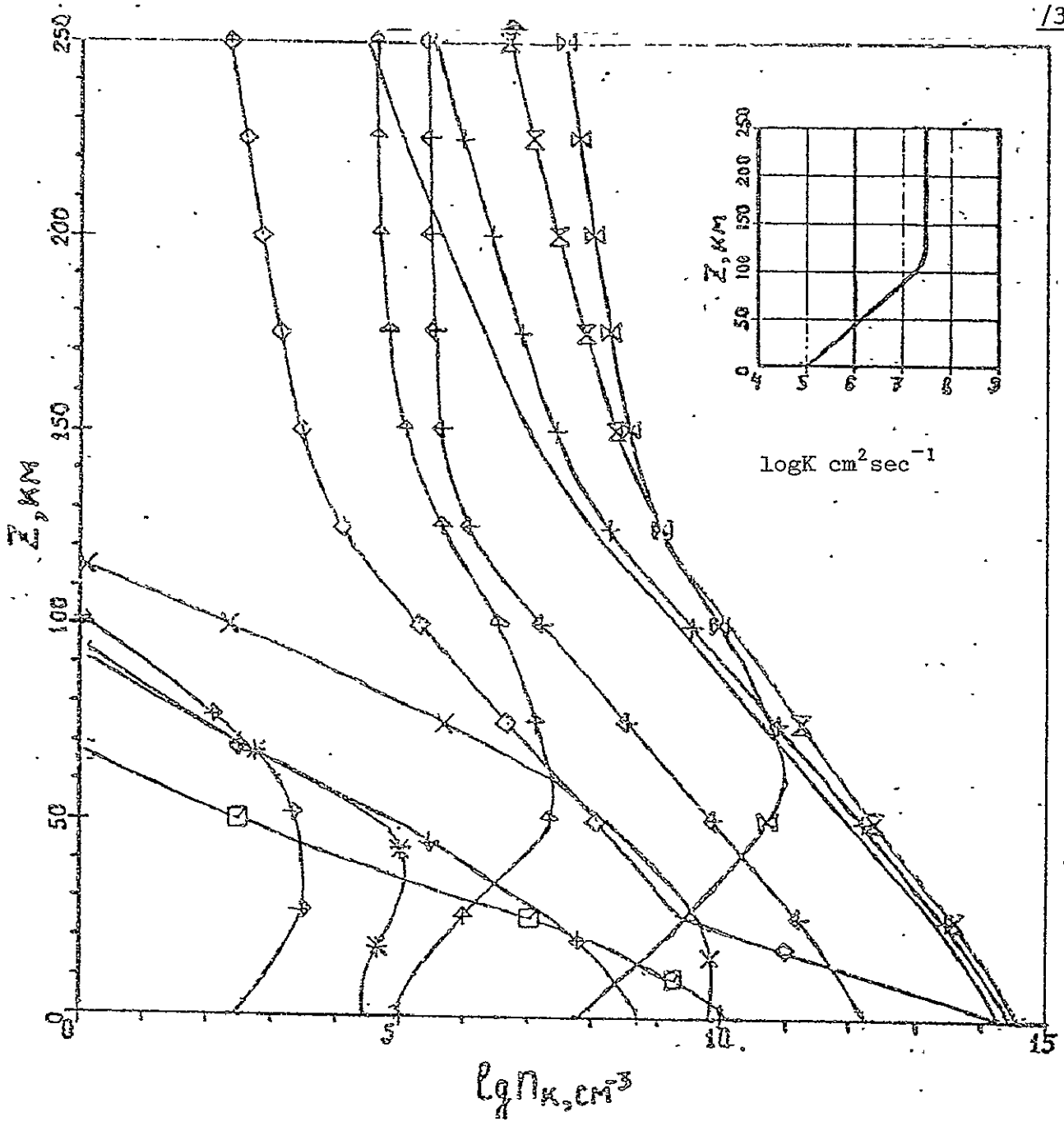

Figure 1. Distribution of the concentrations of the components of the atmosphere of Mars.. Basic variation (variation No.1 in table 2). Notations:

$[CO_2] \cdot 10^{-3}$, + - $[O_2]$, X - $[O_3]$, ◇ - $[H_2O]$, □ - $[H_2O_2]$, ⧖ - $[CO]$,
⋈ - $[O]$, * - $[OH]$, ⍋ - $[H]$, ⍒ - $[HO_2]$, ← - $[H_2]$, → - $[O(^1D)] \cdot 10^3$.

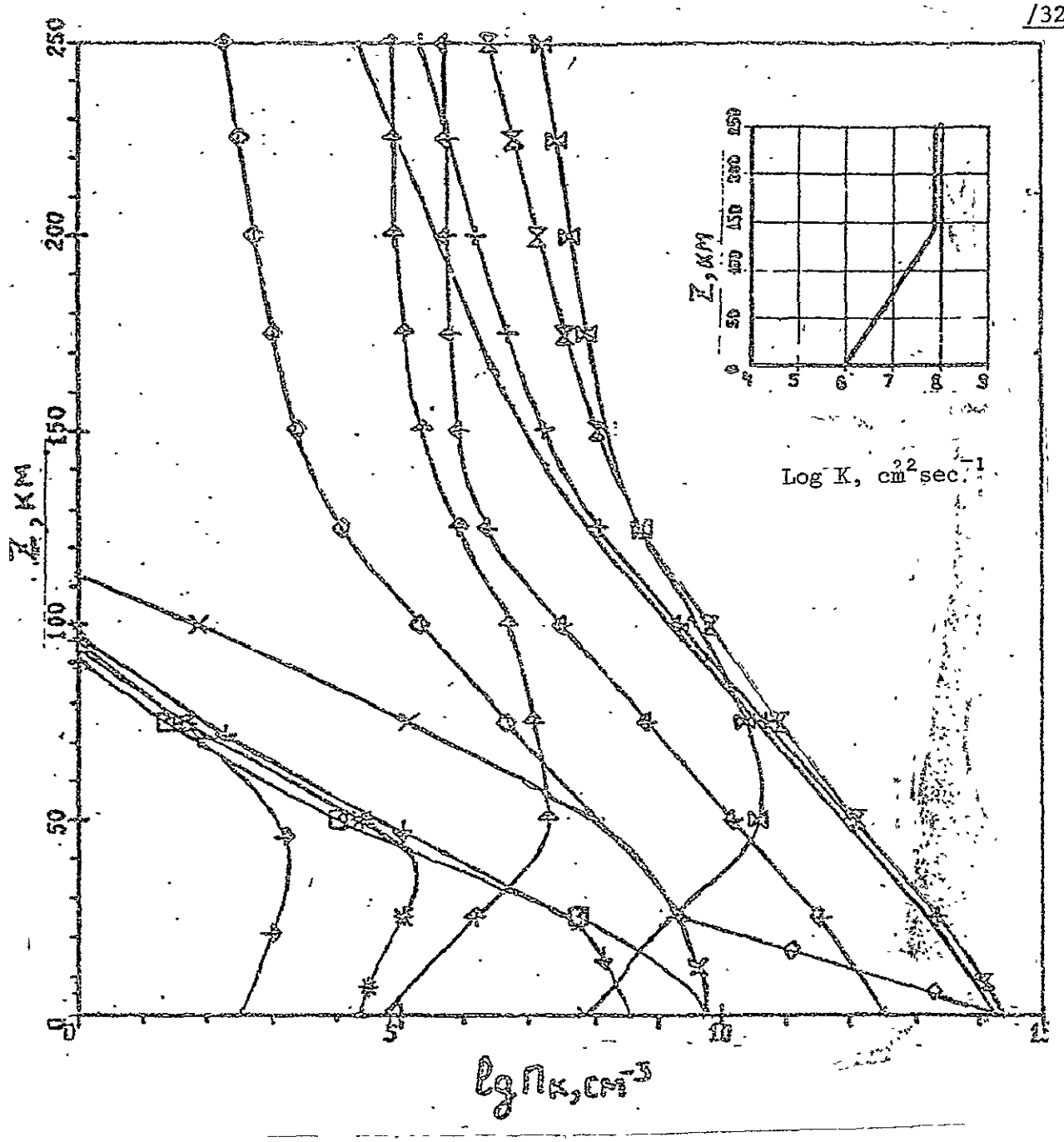

Figure 2. The same as in Figure 1, with maximum turbulence (variation No. 2 in table 2).

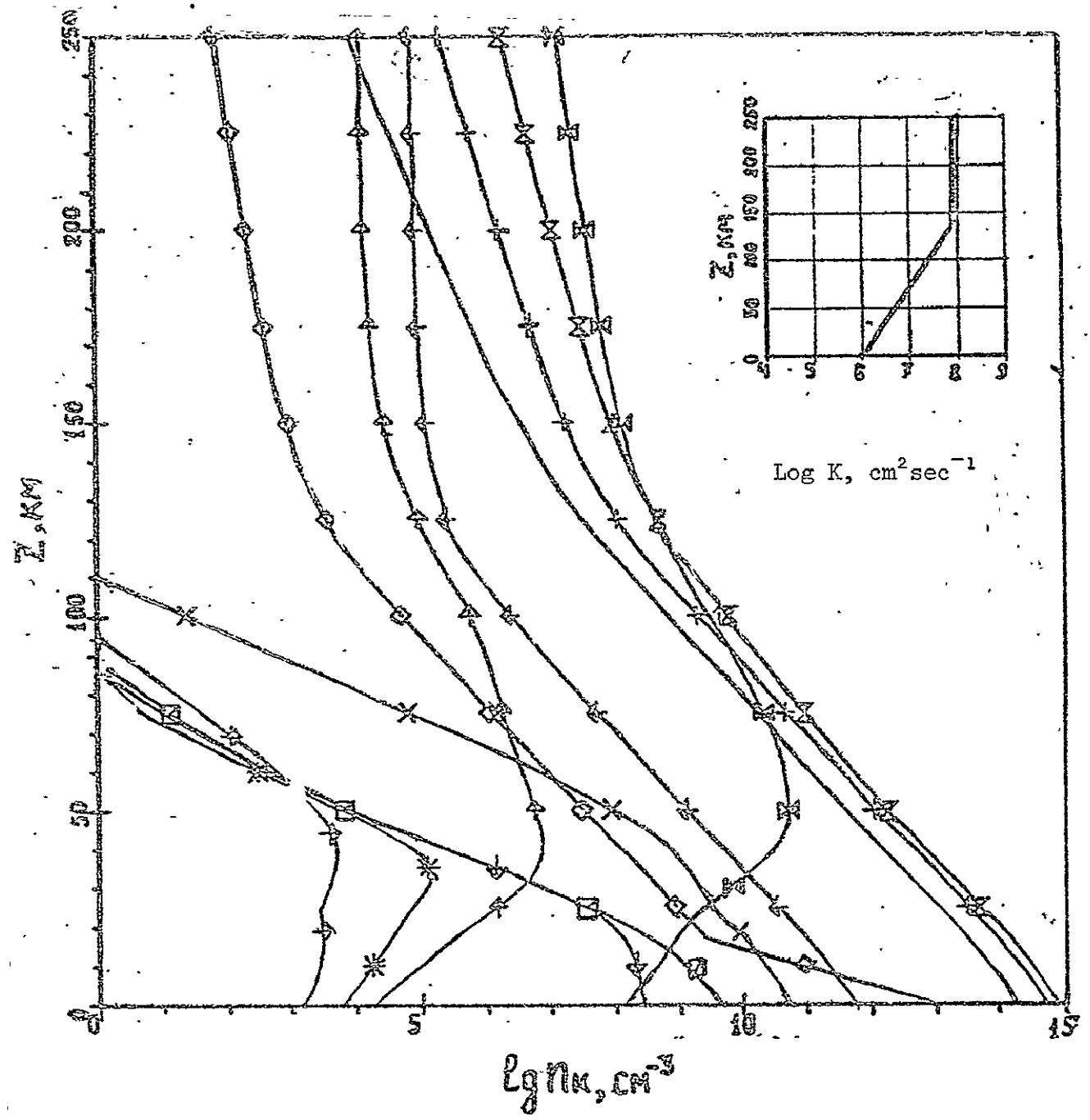

Figure 3. The same as in Figure 1, with minimal moisture - N_{H_2O} - 0.6 μ. of H_2O precipitation (variation No. 4 in table 2).

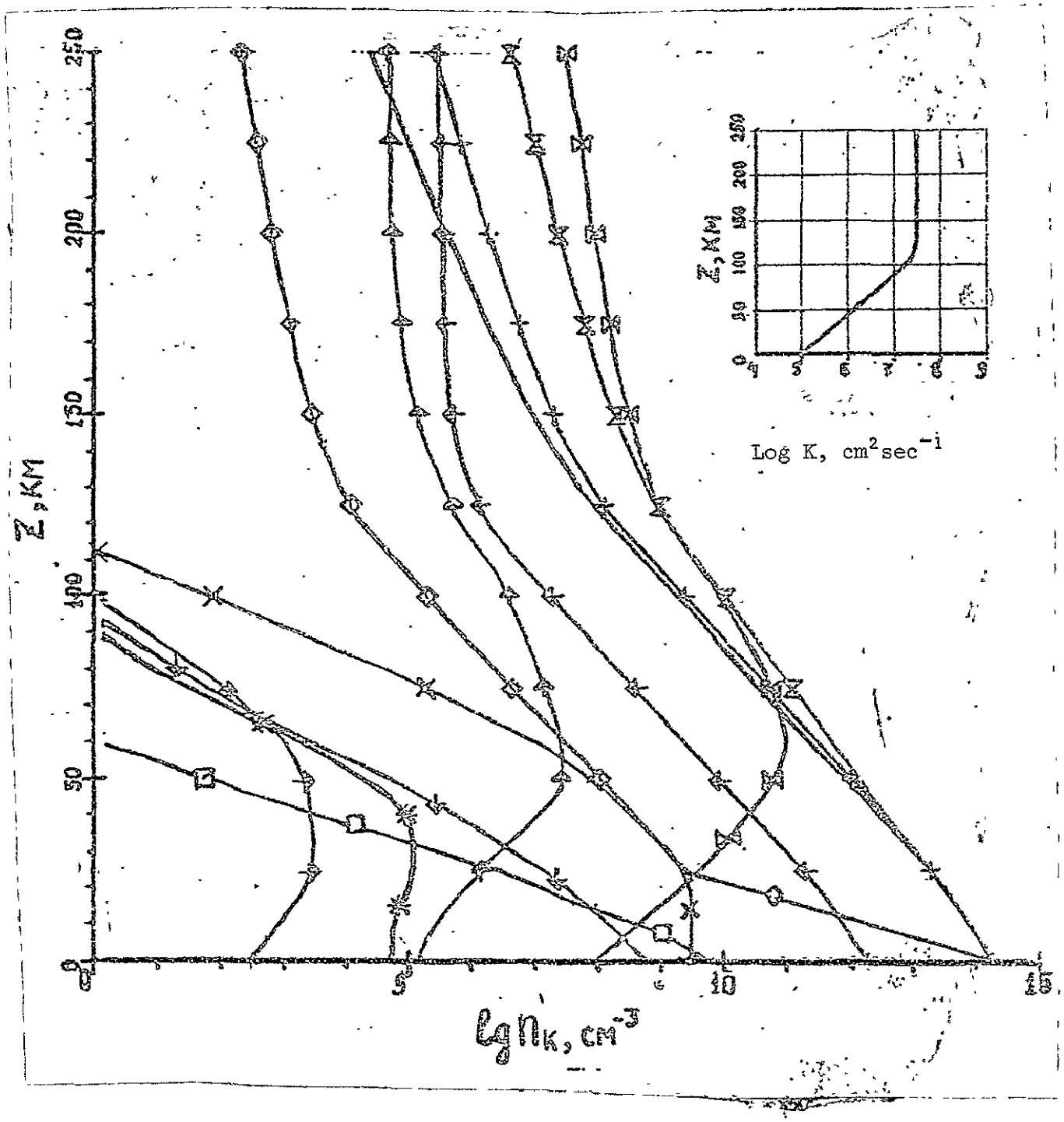

Figure 4. The same as figure 1, with average daily speeds of photodissociation of O_3, H_2O_2 and HO_2 (Variation No. 11 in table 2).

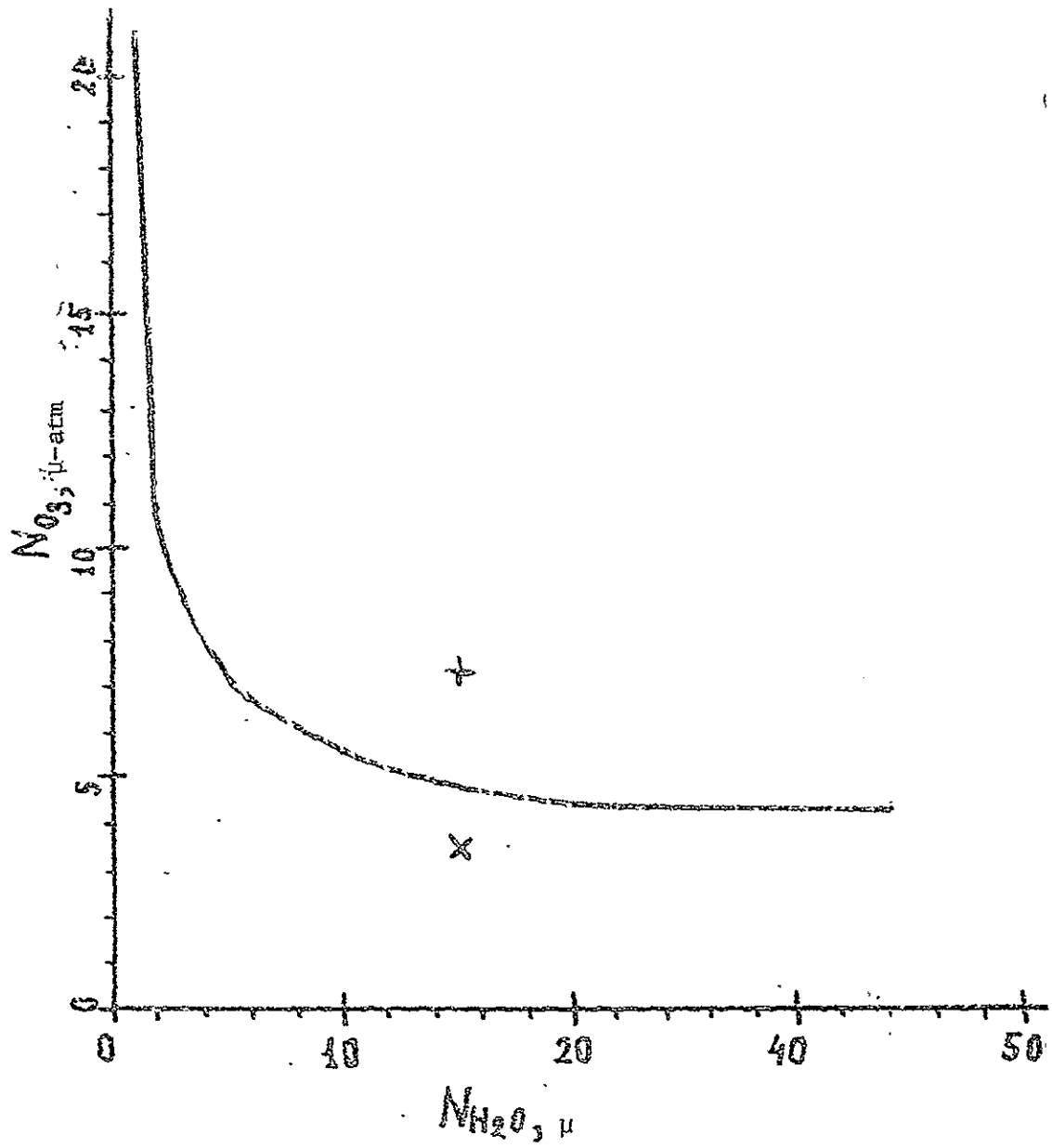

Figure 5. Dependence of the total ozone content on the moisture. The solid curve corresponds to the coefficient of the turbulent mixing in the troposphere $K_o=10^6 cm^2 sec^{-1}$; + - $K_o=10^5 cm^2 sec^{-1}$; x is the average daily speed of photodissociation of O_3, H_2O_2 and HO_2 at $K_o=10^5 cm^2 sec^{-1}$.

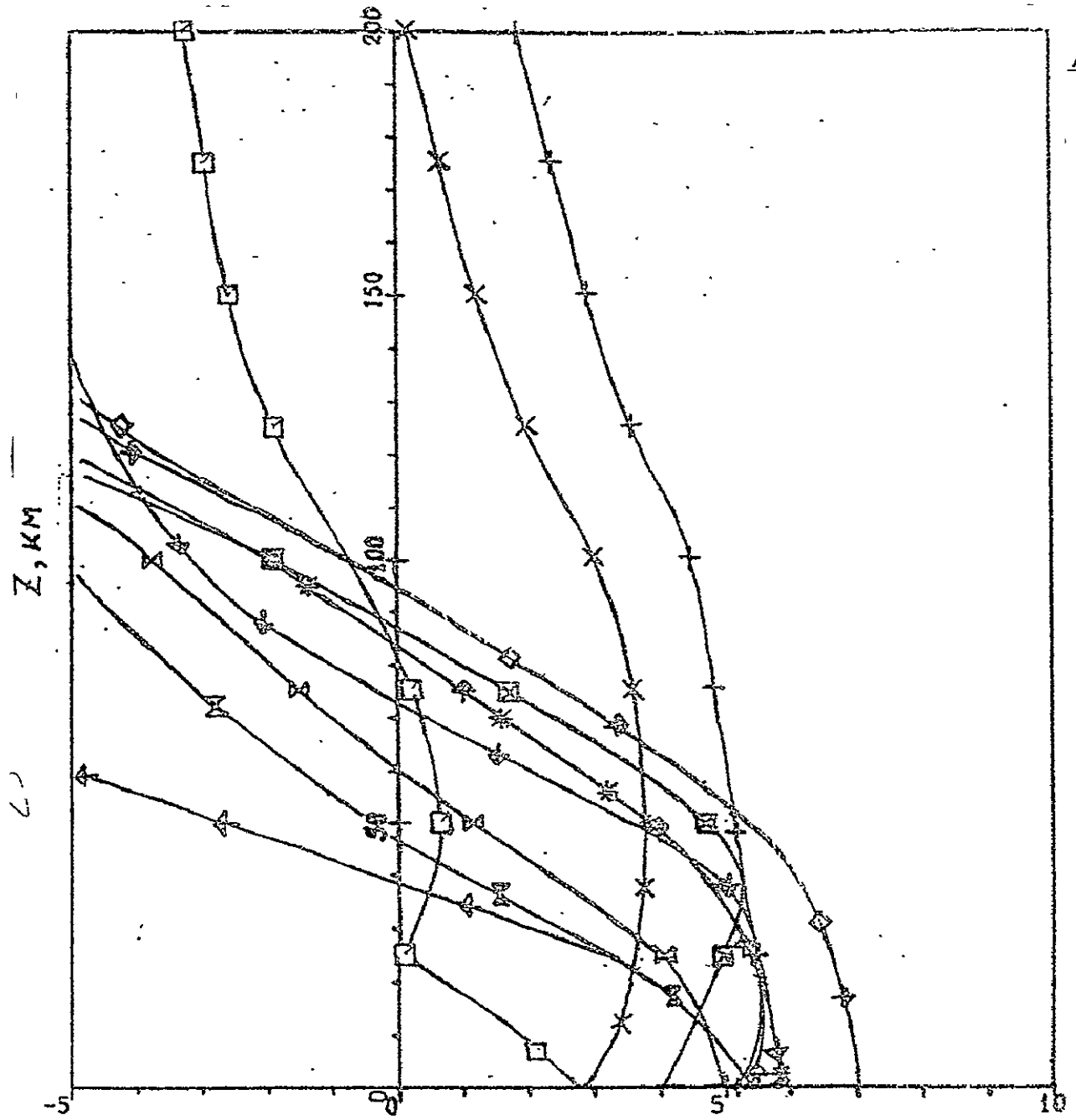

Figure 6. The speed of the basic reactions (variation No. 2 in table 2). Notations: + - the speed of the first reaction, X - 2, ◇ - 3, □ - 4; X - 5, ⋈ - 6, ✳ - 24, ⇑ - 15, ⇓ - 9, ⇐ - 32, ⇒ - 11, ⊠ - 26.

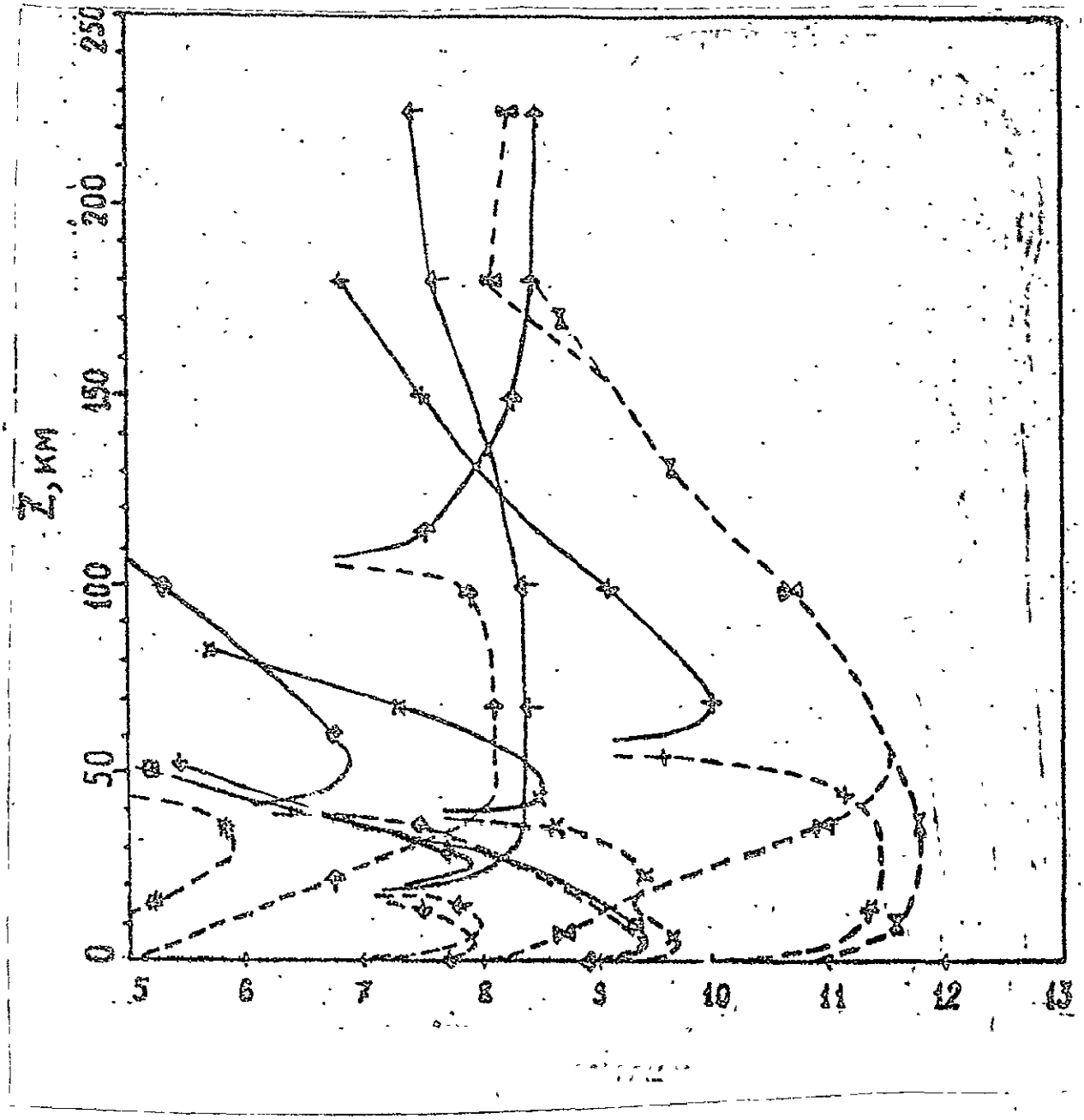

Figure 7. Diffusion streams (variation No. 2 in table 2). Same notations as for figures 1-3.

REFERENCES

1. Barth, C.A., Ann. Rev. Earth and Planet Sci., 1974, 2, 333.
2. McConnell, J.C. in: Phys. and Chem. of Upper Atmospheres, 1973, 309.
3. Moroz, V.I., Ed., Rabochaya model' atmosfery i poverkhnosti Marsa, (Working Model of the Martian Atmosphere and Surface), Preprint, Institute of Space Research, Academy of Sciences, No. 240, 1975.
4. Izakov, M.N., Uspekhi fizicheskikh nauk, 1976, 119, 295.
5. Woiceshyn, P.M., Icarus, 1974, 22, 325.
6. Owen, T., Comments Astrophys. Space Phys., 1974, 5, 175.
7. Owen, T., Bieman K. Science, 1976, 193 (No. 4255), 801.
8. Istomin, V.G., et al, Kosmicheskiye issledovaniya, 1975, 13, 16.
9. Barker, E.S., Nature, 1972, 238, 447.
10. Carlton, N.P., Tranb W.A., Science, 1972, 177, 988.
11. Parkinson, T.D., Hunten, D.M., J. Atmos. Sci., 1972, 29, 1380.
12. Nier, A.O., et al., Science, 1976, 193 (No. 4255), 786.
13. Moroz, V.I., et al., Doklady Academy of Sciences USSR., 1972, 208, 797.
14. Hanel, R.A., et. al., Icarus, 1972, 17, 423.
15. Conrath, B.J., et. al., J. Geophys. Res., 1973, 78, 4267.
16. Moroz, V.I., Nadzhip, A.E., Kosmicheskiye issledovaniya, 1975, 13, 33, 738.
17. Barker, E.S., Icarus, 1976, 28, 247.
18. Barth, C.A., et. al., Science, 1973, 179, 795.
19. Lane, A.L., et. al., Icarus, 1973, 18, 102.
20. Krasnopolskiy, V.A., et. al., Kosmicheskiye issledovaniya, 1975, 13, 37.
21. Kurt, V.G., et. al., Kosmicheskiye issledovaniya, 1973, 11, 315.
22. Dostovalov, S.B., Chuvakhin, S.D., Kosmicheskiye issledovaniya, 1973, 11, 767.
23. Anderson, D.E., Hord, C.W., J. Geophys. Res., 1971, 76, 6666.
24. Anderson, D.E., J. Geophys. Res., 1974, 79, 1513.

25. McElroy, M.B., McConnell, J.C., J. Atmos. Sci., 1971, 28, 879.

26. Thomas, G.E., J. Atmos. Sci., 1971, 28, 859.

27. Strickland, D.J., et. al., J. Geophys. Res., 1972, 77, 4052; 197, 78, 4547.

28. McConnell, J.C., McElroy, M.B., J. Geophys. Res., 1970, 75, 729.

29. Parkinson, T.D., Hunten, D.M., J. Atmos. Sci., 1972, 29, 1380.

30. McElroy, M.B., Donahue, T.M., Science, 1972, 177, 986.

31. Hunten, D.M., Rev. Geophys. Space Phys., 1974, 12, 529.

32. Liu, S.C., Donahue, T.M., Icarus, 1976, 28, 231.

33. Izakov, M.N., Krasitskii, O.P., Geomagnetism i aeronomiya, 16, 209. /24.

34. Izakov, M.N., Morozov, S.K., Kosmicheskiye issledovaniya, 1976, 14, 476.

35. H. E. Hintereger, Ann., Geophys., 1970, 26, 547.

36. M. A. Ackerman, Mesospheric Models and Related Experiments, 1971, 149.

37. R.S. Nakata, et. al., Science of Light, 1965, 14, 99.

38. D. E. Shemansky, J. Chem. Phys., 1972, 56, 1582.

39. R.J.W. Henry, M.B. McElroy, Atmospheres of Mars and Venus, 1968, 251, New York, Gordon and Breach Sci. Publ.

40. Watanabe, K., Advan. Geophys., 1958, 5, 153.

41. Hudson, R.D., Mahle, S.H., J. Geophys. Res., 1972, 77, 2902.

41a. Hasson, V., Nickolls, R.W., Proc. Phys. Soc. L. At. Mol. Phys., 1971, 4, 1789.

42. Watanabe, K., Zelikoff, M., J. Opt. Soc. Amer., 1953, 43, 753.

43. Pankert, T.T., Johnston, H.S., J. Chem. Phys., 1972, 56, 2824.

44. Hochanandel, C.J., et. al., J. Chem. Phys., 1972, 56, 4426.

45. Simonaitis, R., Heicklen, J., J. Chem. Phys., 1972, 56, 2004.

46. Slanger, T. G., et. al., J. Chem. Phys., 1972, 57, 233.

47. Clyne, M.A.A., Thrush, R.A., Proc. Roy. Soc. L., 1972, A269, 404.

48. Vandooren, J., et. al., in "Proceed. 15 Intern. Sympos. on Combustion", 1974, 745.

49. Koufman, F., Ann. Rev. Phys. Chem., 1969, 20, 45.

50. Kaufman, F., Collection "Laboratorniye issledovaniya aéronomicheskikh reaktsii, ("Laboratory Studies of Aeronomic Reactions"), Leningrad, Gidrometeoizdat, 1970.

51. Davis, D.D., et. al., Chem. Phys. Lett., 1973, 22, 273.

52. Baulch, D.L., et. al., Evaluated Kinetic Data for High Temperature Reactions, v. I, 1972, L.

53. Wilson, W.E., J. Phys. Chem. Ref. Data, 1972, 1, 535.

54. Lloyd, A.C., Intern. J. Chem. Kinet., 1974, 6, 169.

55. Albers, E.A., et. al., "Proceed. 13 Internat. Sympos. on Combustion", 1971, 81.

56. Young, R.A., et. al., J. Chem. Phys., 1967, 47, 228.

57. Cvetanovic, R.J., Canad. J. Chem., 1974, 52, 1452.

58. Anderson, L.G., Rev. Geophys. Space Phys., 1976, 14, 151.

59. Baulch, D.L., et. al., High Temp. Reactions Rate Data, 1969, 3, 18.

60. Hampson, R.F., J. Phys. Chem. Ref. Data, 1973, 2, 267.

61. Anderson, J.G., Kaufman F., Chem. Phys. Lett., 1973, 19, 483.

62. Greiner, N.R., J. Phys. Chem., 1968, 72, 406.

63. Girshfelder, Dzh., Curtis, Ch., Bird, P., Molekularnaya teoriya gazov i zhidkostey, (Molecular Theory of Gases and Liquids), Moscow, Izdatelstvo Inostrannoy Literatury, 1961.

64. Chapman, S., Cowling, T., Matematicheskaya teoriya neodnorodnykh gazov, (Mathematical Theory of Heterogeneous Gases), Moscow, 1960.

65. Vargaftik, N.B., Spravochnik po teplofizicheckim sv-vam gazov i zhidkostei, (Booklet on the Thermo-Physical Properties of Gases and Liquids), Moscow, 1972.

66. Mason, E.A., Marrero, T.R., Adv. Atom. Molec. Phys., 6, 1970, 155.

67. Izakov, M.N., Kosmicheskiye issledovaniya, 1977, 15, 248.

68. Golitsyn, G.S., Vvedeniye v dinamiku planetnykh atmosfer, (Introduction to the Dynamics of the Planetary Atmospheres), Leningrad, Gidrometeoizdat, 1973.

69. Hess, S. L., Icarus, 1976, 28, 269.

70. McElroy, M.B., Science, 1972, 175, 443.

71. Samarskii, A.A., Vvedeniye v teoriyu paznostnykh skhem, (Introduction to the Theory of Differential Schemes), Moscow, 1971, P. 131, "Nauka".

72. Kulikov, Yu.N., Preprint, In-ta prikladnoy matematiki, 45, 1976.

73. R.P. Turco and R.C. Whitten, J.P.R., 79, 3179.

74. T.S. Shimazaki, T. Ogawa, J.G.R., 1974, 79, 3412.

75. Kieffer, H.H., et. al., Science, 1976, 193, (No. 4255), 780.

76. Izakov, M.N., Krasitskii, O.P., Morozov, S.K., Kosmicheskiye issledovaniya, 1976, 14, 585.